CHAPTER 4

EFFECT OF SOLVENT, PARTICLE SIZE AND SUBSTRATE ON THE BREATH FIGURES OF HYBRID FILM

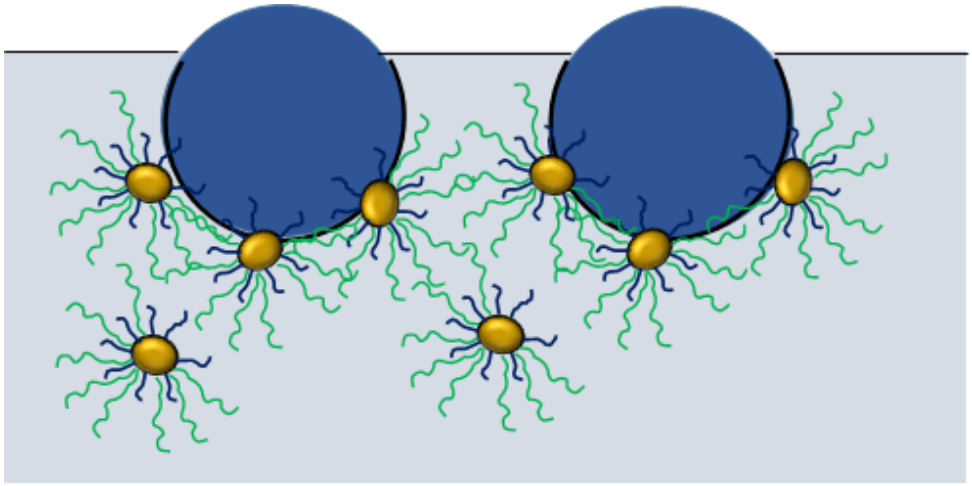

4.1. ABSTRACT

In this chapter, the influence of solvent, particle size, and the substrate on the breath figure (BF) morphology is discussed. Tetrahydrofuran (THF), chloroform (CFM), carbon disulphide (CS2), and dichloromethane (DCM) were used as solvents. The dispersion characteristics of the amphiphilic alumina (SA) particles in the solvents have been evaluated. The influence of particle size on the BF patterns has been evaluated using alumina particles having average particles size of 20nm and comparing the results using particles size of 100nm in the chapter 3. BF patterns from CFM also produced using polypropylene (PP) film as the substrate under the same experimental condition employed for producing BF patterns using the glass substrate.

4.2. INTRODUCTION

Various factors such as humidity, temperature, polymer characteristics (type, molecular weight, and concentration), solvent used for preparing solutions/suspensions can affect the breath figure formation and the morphology of the patterns. The solvent used to dissolve the polymer plays a major role in all most all process involved in the BF formation (*Servoli et al., 2010; Ferrari et al., 2011*). Various solvent parameters such as evaporation rate, density, vapour pressure, miscibility with water, thermodynamic compatibility with the polymer matrix, etc. can influence the BF morphology. For example, linear polystyrene (PS) produced BF patterns with chloroform and dichloromethane while PS was BF incompatible with solvents like THF and ethyl acetate. Some reports demanded the necessity of water immiscibility while some other reports indicated that immiscibility is not an essential condition (*Yi Wu et al. 2008*). In inorganic particle-assisted BF patterns, dispersion of the hydrophilic particles in the hydrophobic solvents has to be considered in order to predict the BF morphology.

Another important influencing parameter for the particle-assisted BF formation is the size of the particles. Pieranski (*Pieranski, 1980*) studied the interfacial behaviour of colloidal particle and related the energy 'E' required to remove a single colloidal particle from the interface by the following equation

$$\boldsymbol{E = \pi R^2 \gamma_{wo} (1 - |\cos\theta|)^2} \text{---------- (4.1)}$$

Where 'R' refers to the particle radius, $'\gamma'_{wo}$ is the water/oil interfacial tension, 'θ' represents the contact angle measured through the water phase. The energy required to remove a particle from the interfaces in an emulsion is directly related to the radius of the particles. Recently, Sun et al. reported (*Sun et al., 2010*) that the regularity of

the BF patterns were improved with the particle size. Experiments conducted using particles of different size ended up in a conclusion that although particles having higher size are expected to promote a regular breath figure formation, there is no competitive preference for the adsorption of the particles having different size at the BF interface. Particles with larger size only have the advantage to be adsorbed at the interface while finer particles are easily carried along with the droplets towards the three phase contact line thereby, arresting the coalescence of the water droplets. The substrate also has a marked influence in deciding the BF morphology. Different substrates produced different BF patterns under the same conditions. Linear polystyrene forms regular patterns with CS_2 on the glass substrate, while it fails to achieve uniform patterns in PET films (*Ghannam et al., 2007*). However, the hydrophilicity, wettability, and affinity of the substrate with the polymer affect the BF morphology. Above all, the role of substrate in the overall BF mechanism is strictly related to the solvent used.

In this chapter, the effect of dispersion characteristics of amphiphilic alumina (SA) particles in different solvents, particle size of 20nm and polypropylene substrate are discussed

4.3. RESULTS AND DISCUSSIONS

4.3.1. Effect of solvent on BF Pattern Morphology

Aprotic polar solvents such as tetrahydrofuran (THF) and dichloromethane (DCM), and nonpolar solvents such as chloroform (CFM) and carbon disulphide (CS2), were used to study the effect of solvent. Amphiphilic alumina particles (SA particles) which were referred as 2SA, 2.6SA and 4SA particles (chapter 2) were used for preparing suspensions in polystyrene (PS) solutions (PSA suspensions) for

preparing BF patterned films. The particle concentration in the suspensions was fixed at 3 wt %, which is the dispersion loading limit of the particles in PS matrix. The patterned hybrid films were prepared as described in 3.3.2 and referred as P3(ySA), where y represents the Hb/Hp ratio of the SA particles. Various properties of solvents influencing the BF formation and BF pattern are listed Table 4.1.

Table 4.1. Properties solvents selected for BF formation

Solvents	**density @20°C (g/cm3)**	**viscosity @25°C (mPa s)**	**solubility in water @ 20°C (g/100 mL)**	**interfacial tension with water@ 25°C (mN/m)**	**boiling point (°C)**	**vapor pressure @25°C (kPa)**
THF	0.8892	0.456	Miscible	-	65	21.6
CFM	1.4832	0.537	0.8	33.5	61	26.2
CS2	1.2632	0.352	0.22	48.1	46	48.2
DCM	1.3266	0.413	2	28.3	40	58.2

The Formation and morphology of BF patterns in the hybrid films using THF as solvent was discussed in chapter 3 and the results are incorporated here for comparative study. The BF patterns produced on the hybrid films from THF, CFM, CS2 and DCM are shown in figures 4.1 to 4.4 respectively. The BF cavity size, feature density (cavity/cm^2), and conformational entropy of these hybrid films measured using imagej software are summarized in Table 4.2 (a-d).

As discussed in chapter 3, BF morphology of the drop-cast hybrid films from THF varied with the Hb/Hp ratio of the particles such a way that uniform patterns with high feature density was attained for P3(2.6SA) hybrid film (figure 4.1B).

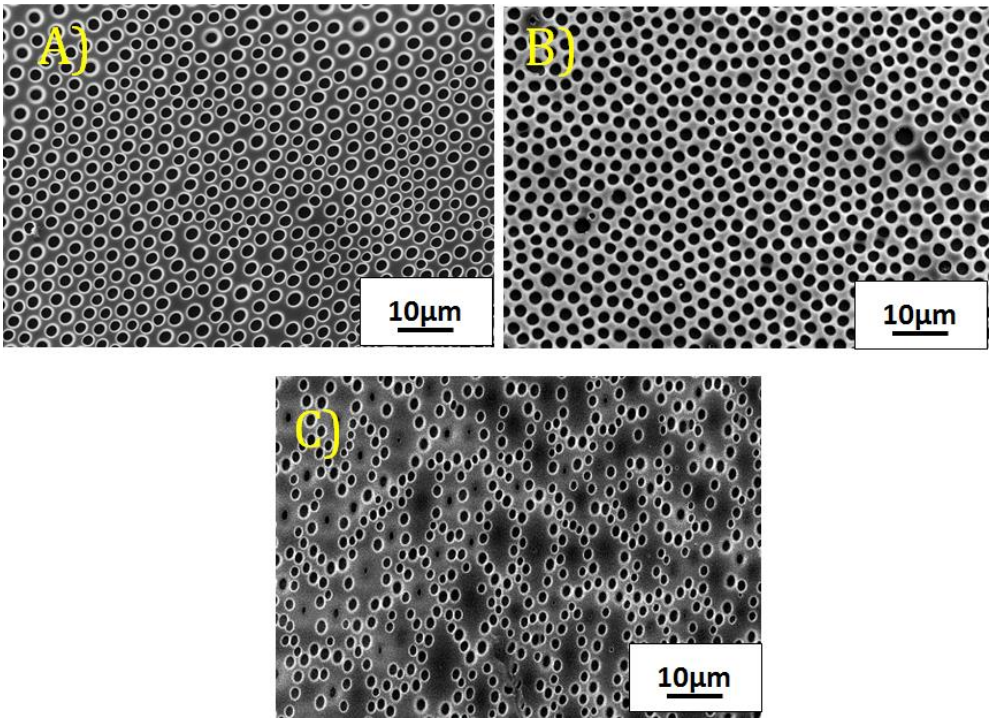

Figure 4.1. SEM images of BF patterned PSA hybrid films (a) P3(2SA), (b) P3(2.6SA) and (c) P3(4SA) produced using THF

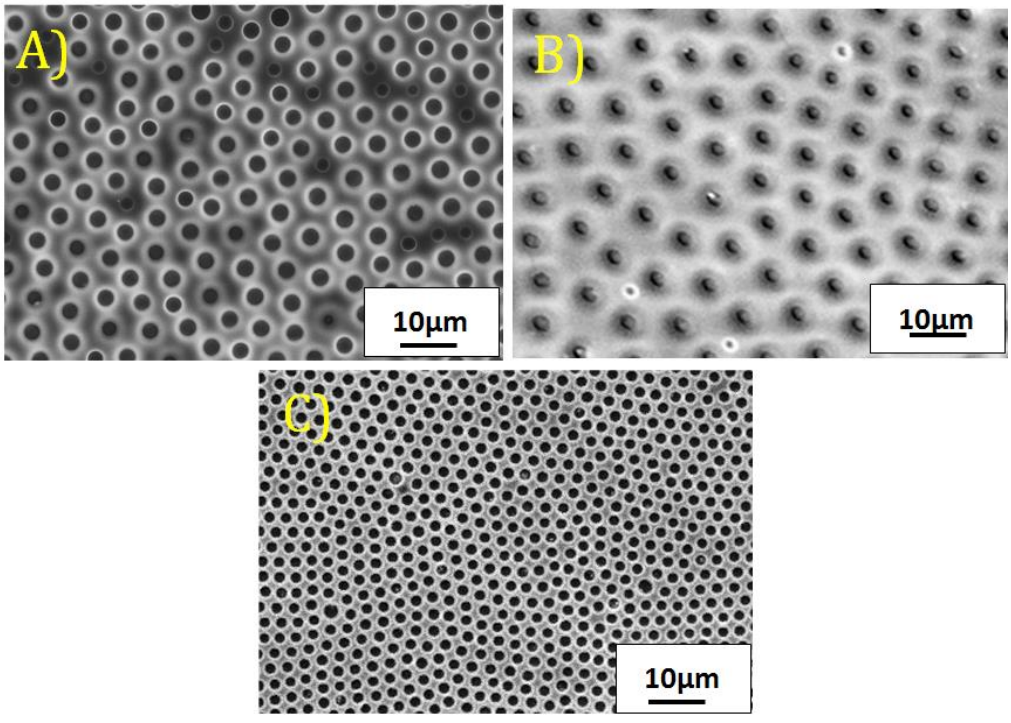

Figure 4.2. SEM images of BF patterned PSA hybrid films (a) P3(2SA), (b) P3(2.6SA) and (c) P3(4SA) produced using Chloroform

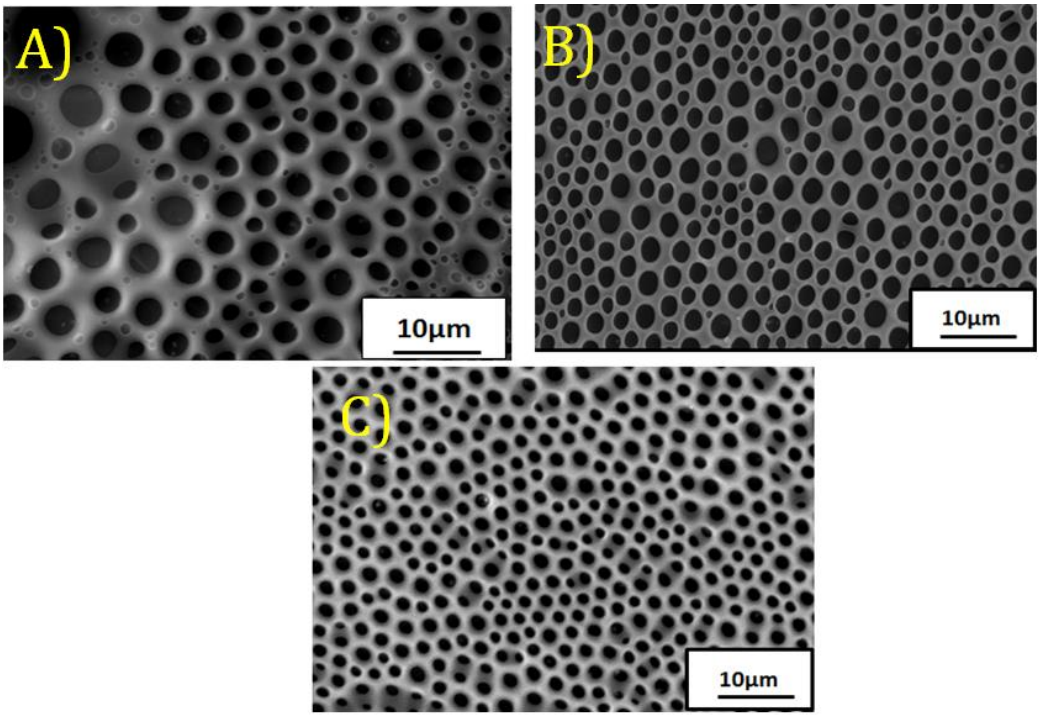

Figure 4.3. SEM images of BF patterned PSA hybrid films (a) P3(2SA), (b) P3(2.6SA) and (c) P3(4SA) produced using Dichloromethane (DCM).

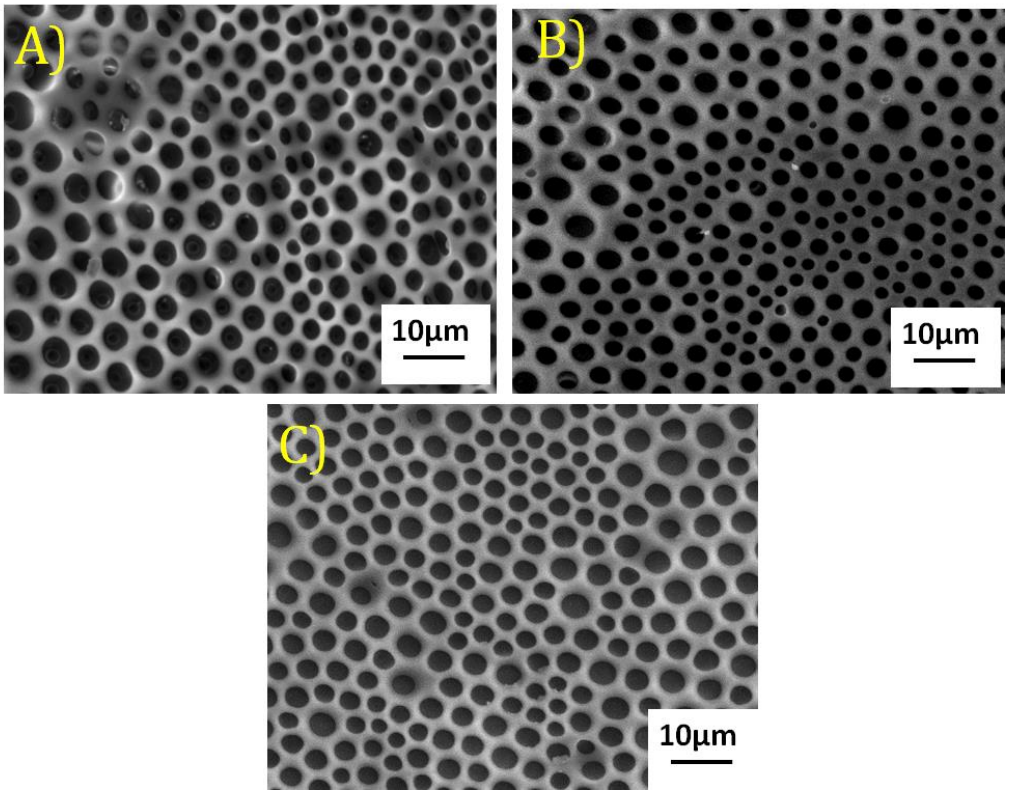

Figure 4.4. SEM images of BF patterned PSA hybrid films (a) P3(2SA), (b) P3(2.6SA) and (c) P3(4SA) produced using Carbon disulphide (CS2).

Table 4.2a. BF cavity size, feature density and conformational entropy of PSA hybrid films using THF

Composite	Cavity size (μm)	Feature density (Cavity/cm^2)	Conformational Entropy(S)
P3(2SA)	1.66±0.08	14x10^7	0.77
P3(2.6SA)	1.61±0.09	15 x10^7	0.68
P3(4SA)	1.56±0.26	6.1 x10^7	-

Table 4.2b. BF cavity size, feature density and conformational entropy of PSA hybrid films using CFM

Composites	Cavity size (μm)	Feature density (Cavity/Cm^2)	Conformational Entropy (S)
P3(2SA)	3.30 ±0.14	3.0 x10^7	-
P3(2.6SA)	1.70±0.06	5.0 x10^7	0.64
P3(4SA)	1.50±0.04	16 x10^7	0.46

Table 4.2c. BF cavity size, feature density and conformational entropy of PSA hybrid films using CS2

Composites	Cavity size (μm)	Feature density (Cavity/Cm^2)	Conformational Entropy (S)
P3(2SA)	2.9±1.04	4.1 x 10^6	-
P3(2.6SA)	2.2±0.37	1.2 x 10^7	-
P3(4SA)	1.5±0.21	1.5 x 10^7	0.74

Table 4.2.d. BF cavity size, feature density and conformational entropy of PSA hybrid films using DCM

Composites	Cavity size (μm)	Feature density (Cavity/cm^2)	Conformational Entropy (S)
P3(2SA)	4.2±0.93	0.26×10^7	0.97
P3(2.6SA)	3.8 ±0.71	0.30×10^7	0.89
P3(4SA)	4.0 ±0.43	0.26×10^7	0.80

Whereas, BF patterns from chloroform followed a different trend. The pore size decreased, uniformity and feature density of BF patterns increased with the hydrophobicity of the SA particles. P3(2SA) film (figure 4.2A) showed an irregular pattern with average pore size of 3.3μm, while the pore size decreased to 1.7 μm for P3(2.6SA) film (figure 4.2B) and then to 1.5 μm for P3(4SA) film (figure 4.2C). On comparing the BF patterns on P3(2.6SA) and P3(4SA) films, it can be seen that the pore interval decreased with the hydrophobicity of the particles which remarkably increased the feature density (from 3×10^7 to 16×10^7/cm^2) of the pattern. Similarly, the conformational entropy ('S' the measure of regularity of the pattern) decreased from 0.64 to 0.46. Lowest pore size, highest feature density and pore order was obtained for P3(4SA) hybrid film.

The BF patterns produced on the hybrid films from CS2 followed an analogous observation as that of from CFM. The pattern produced in P3(2SA) hybrid film (figure 4.3A) appeared like large circular cavities (1.9-3.9μm) with varying size and depths as defined by large standard deviation. The size distribution became narrower such that the pattern with regularity maximum was produced by P3(4SA) (figure 4.3C) for which the average cavity size, feature density and conformation entropy measured

were 1.5±0.22 μm, $1.5x10^7$ features/cm^2 and of 0.74 respectively. However, the cavities in P3(2SA) showed wide size distribution. The cavities appeared to be in different levels, which was more prominent in P3(4SA), possibly due to 00shrinkage stresses during drying owing to the high evaporation rate of CS2**.**

In contrast to the above results, the hybrid films from DCM exhibited totally different pattern. The cavity size of all the three films remained almost same with an average value of 4μm. Specifically, the average BF cavity size of P3(2SA), P3(2.6SA) and P3(4SA) films were 4.2±0.93 μm, 3.8 ±0.71 μm and 4.0 ±0.43 μm respectively. However, the uniformity of the patterns improved slightly with the hydrophobicity of the particles such that the conformational entropy decreased from 0.97 to 0.80. However, as observed for films from CS2, the cavities were of wide size distribution and found at different levels, which was more prominent in P3(2SA).

The morphological variation of the patterned film with the Hb/Hp value of the SA particles and the solvent can be explained on dispersion characteristics of the particles in the solvents as well as its mobility from the solvent to the solvent/water interface. As discussed in chapter 3, uniform patterns from THF were produced with SA particles having Hb/Hp ratio of ~2.6. The high hydrophobicity with 4SA particles retarded its ability to migrate from the solvent towards the water droplet/solvent interface in the case of THF. All the above said particles (2SA, 2.6SA, and 4SA) exhibited nearly identical dispersion characteristics (chapter 2). The phenomenon was explained based on the polar nature and miscibility of the solvent with water. The combined effect of electrostatic and steric assisted dispersion demanded a low Hb/Hp value for the amphiphilic particles to produce a uniform BF pattern.

In contrast to THF, CFM is a non-polar and water immiscible solvent. The electrostatic assisted dispersion can be completely ruled out. Dispersion of the amphiphilic particles occurred by the steric repulsion from the PS segments. Hydrophobicity of the particles increased with the PS content (length of the PS segments increased in the present amphiphilic particles). The increased segment length promoted steric aided dispersion of the particles. The hydrophilic amino moiety promoted the capillary movement of particles towards the BF interface. The water immiscible nature of chloroform created a sharp boundary at the interface where the particles align with its hydrophilic amino part into the water phase and the hydrophobic PS segments associated with the particles into the solvent phase. The influence of Hb/Hp value on dispersion of the amphiphilic particles in PS/CFM solution was evident from the DLS analysis of the suspensions (see section 2.4.3). The particle-agglomerate size in the suspension decreased in the order of 2SA>2.6SA>4SA. Fine dispersion of 4SA particle resulted in the availability of more particle domains for stabilization of fine water droplets during BF formation which resulted in pore size minimum and feature density maximum of the pattern for P3(4SA).

As mentioned earlier, the morphological change in hybrid films from CS2 followed the same trend as that observed for the film from CFM. Obviously, the particle-agglomerate size in the suspension decreased in the order of 2SA>2.6SA>4SA, as was evident from DLS data (chapter 2). As a result, P3(4SA) system produced the most uniformly patterned films among the other two systems.

On comparing the BF patterns formed on P3(4SA) hybrid film from CFM with that from CS2, it can be seen that both the films showed an average cavity size of 1.5

μm. On the other hand, the feature density and regularity were remarkably high for the hybrid film from CFM. The same can be explained as following. From table 4.1, it can be seen that CS2 exhibited higher value of vapour pressure (48.2 kPa) than CFM (26.2 kPa). As a result, the air surrounding the PSA/CS2 drop-cast get saturated with the CS2 vapour faster than that of PSA/CFM drop-cast. Therefore, the evaporation of CS2 produced lower temperature gradient between the solution surface and the surroundings than that produced by CFM. This caused formation reduced amount of water droplets on the PSA/CS2 drop-cast surfaces (*Ma et al., 2011*). This led to larger separation between the stabilized droplets/cavities and thereby, diminished feature density and regularity of the pattern.

The hybrid films from DCM followed a totally different trend. The films exhibited relatively high pore size (~4 μm) and low feature density (0.26 x10^7 /cm^2). Although DCM is a chlorine containing solvent just like CFM, the dielectric constant of the former (8.9 at 25 °C) is higher than that of the later (4.8 at 25 °C). Moreover, DCM has a very low boiling point of 40 °C and high vapour pressure of 58.2 kPa. The high vapour pressure of DCM enormously decreased the evaporation rate of the solvent (relative evaporation rate of DCM with respect of n-butyl acetate is 7, that of CFM and CS2 are 11.6 and 22.6 respectively) and hence the water condensation on the drop-cast surface is reduced. Since the particle assisted BF mechanism is operating in these systems, the interaction of the amphiphilic alumina particles with the solvent has to be considered with prime importance. According to the classification based on Hansen solubility parameter (*Hansen, 2007*) DCM is regarded as a polar aprotic solvent with low miscibility with water. The parameter corresponding to the dipolar intermolecular force (δP) between the DCM molecules

is 7.3, which is higher than THF (δP=5.7). Therefore, the PS associated with SA particles showed comparatively good solubility in DCM. Also, the DCM solvated amino group on the SA particles reduced the adsorption capability of SA particles in DCM/water interface. This caused a delay in stabilization of the water-droplets which favoured growth of the droplets. This along with reduced number of water droplets due to reduced water condensation resulted in high cavity size and low feature density. Unlike THF, DCM is immiscible with water. A thin boundary exists between DCM and water droplets. SA particles get adsorbed in this interface with the amino group towards the more hydrophilic water phase. In other words, the adsorption capability of the SA particles at DCM/water interface was insensitive to the polymer content. Therefore, the hybrid films using 2SA, 2.6SA and 4SA particles exhibited close values for cavity size, feature density and conformational entropy.

Figure 4.5 shows the magnified SEM image of the film from DCM. A close examination the cavities revealed the formation of a ring structure by the particles at the bottom, indicating the formation of through-pore structure. The bottom portion of the droplets up on reaching the substrate surface, failed to produce the through pore structure. The particles along with the polymer in the failed portion formed a ring structure along the contact line of the cavity with the glass plate.

On comparing the BF patterns obtained from the four solvents, the most uniform BF pattern from THF was yielded for P3(2.6SA) film while P3(4SA) produced the most uniform pattern from other three solvents. According to our results, the state of dispersion of the amphiphilic-particles in different solvents is a key parameter for the BF morphological variation. Moreover, other solvent characteristics such as water miscibility, polarity, vapour pressure, solvent/water

interfacial tension, affinity between the amphiphilic-particles and the solvent, etc. also have to be considered. For example, the miscibility of THF with water is responsible for the slightly higher BF cavity produced on its hybrid films whereas in DCM, the low evaporation rate of the solvent and the increased interaction between the SA particles and DCM were cumulatively contributed to the unusually high cavity size.

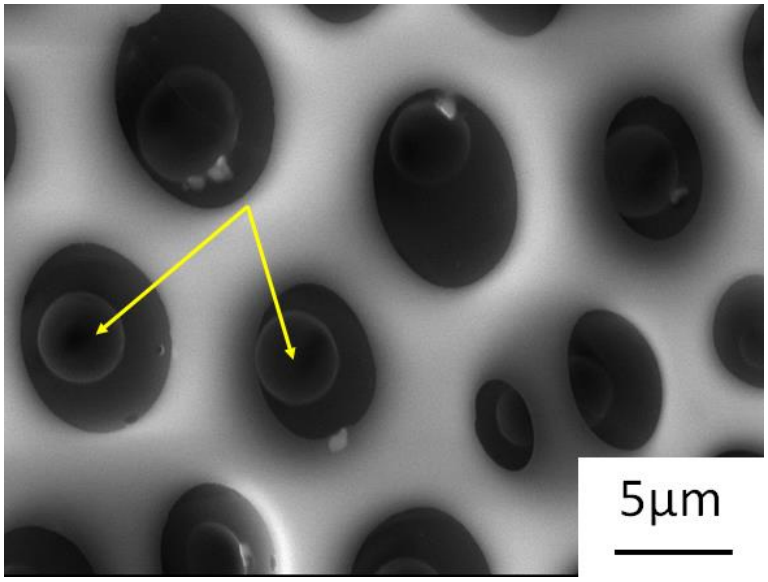

Figure 4.5. Magnified SEM images of micropatterned hybrid films from DCM

4.3.2. Effect of Particle Size on BF Pattern Morphology

The effect of particle size on BF morphology was investigated using alumina particle having an average size of 20 nm for preparing BF patterns and comparing the results with the results obtained using particles of average size of 100nm. Figure 4.6 shows the TEM image of the particles. These particles were amphiphilic modified by silane treatment with AS/VS mixture followed by *in-situ* polymerization with styrene as described in section 2.3.2. However, the silane-treated particles (A20) which were synthesised using 3 wt. % silane mix with respect to alumina showed

poor dispersion in organic solvents such as tetrahydrofuran, chloroform, carbon disulphide, etc. due to its high surface area. Therefore, 7 % of the silane mix was used for the treatment. However, S/A molar ratio of 0.1 was used for polystyrene modification. These amino functionalised amphiphilic-alumina particles were referred as SA20.

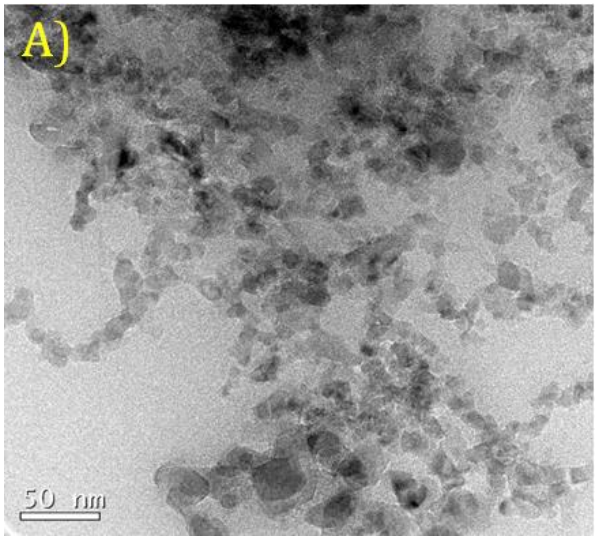

Figure 4.6. TEM image of alumina having average particle size of 20nm

The BF patterned hybrid films were fabricated using the suspensions obtained by dispersing the particles in polystyrene/THF solution of concentration of 15 mg/mL, same as that used for preparing SA100. The particle loading was varied from 0.5 to 2 wt %. These PSA suspensions were drop-casted on a glass substrate and allowed to dry under ambient conditions (temperature of ~30°C and humidity of 70-80%). The patterned hybrid films prepared were referred as Px(SA20), where x represents the particle loading.

Figure 4.7 shows the thermogram of A20 and SA20 particles. The loss due to organic associated with silane and that of polystyrene content associated with the particles through vinyl group were 5.7%. and 6.4% respectively.

The corresponding Hb/Hp balance of the particles (see chapter for the calculation) was ~3. Although the Hb/Hp balance of SA20 was comparable with the SA100, these particles showed little dispersion in non-polar solvents. This might be due to the high surface area and hydrophilicity of the particles as a whole in comparison with the modifier hydrophobicity due to the unreacted hydroxyl group present on the particle surface

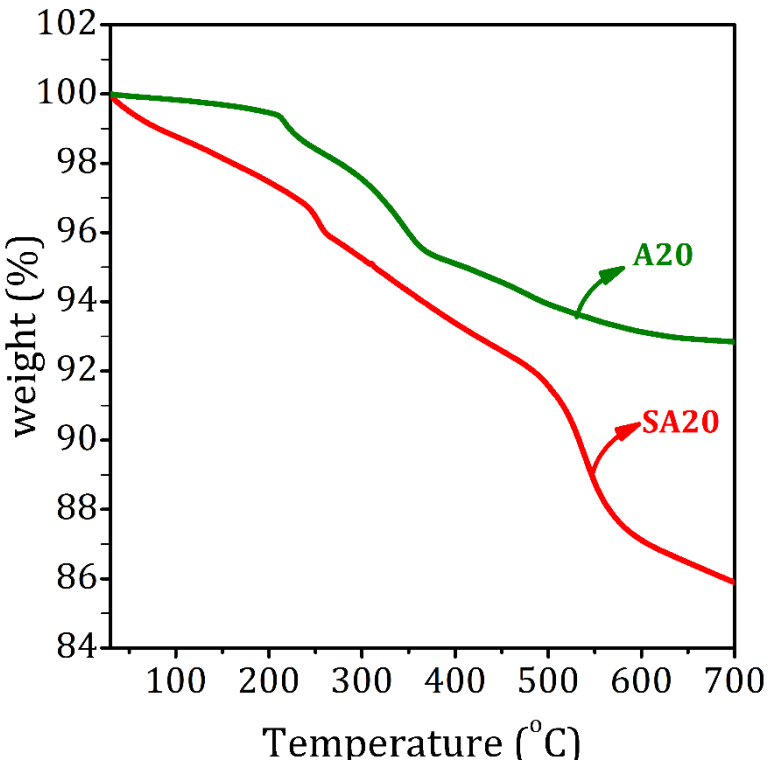

Figure 4.7. TG curves of A20 and SA20 particles

. Figure 4.8 shows the SEM images of the drop-cast residues of PSA/THF suspensions of SA20 particles, where the particle concentration was varied from 0.5 to 2wt% with respect to the PS content. The residues are referred as P0.5(3SA20), P1(3SA20) and P2(3SA20) hybrid films. It can be seen that P0.5(SA20) exhibited relatively uniform BF pattern when compared to that by P1(SA20) and P2(SA20). The average cavity size, feature density and conformational entropy of the pattern

measured using imagej software were 3.1 ±0.12 µm, 5.8× 10^7/cm^2 and 0.60 respectively.

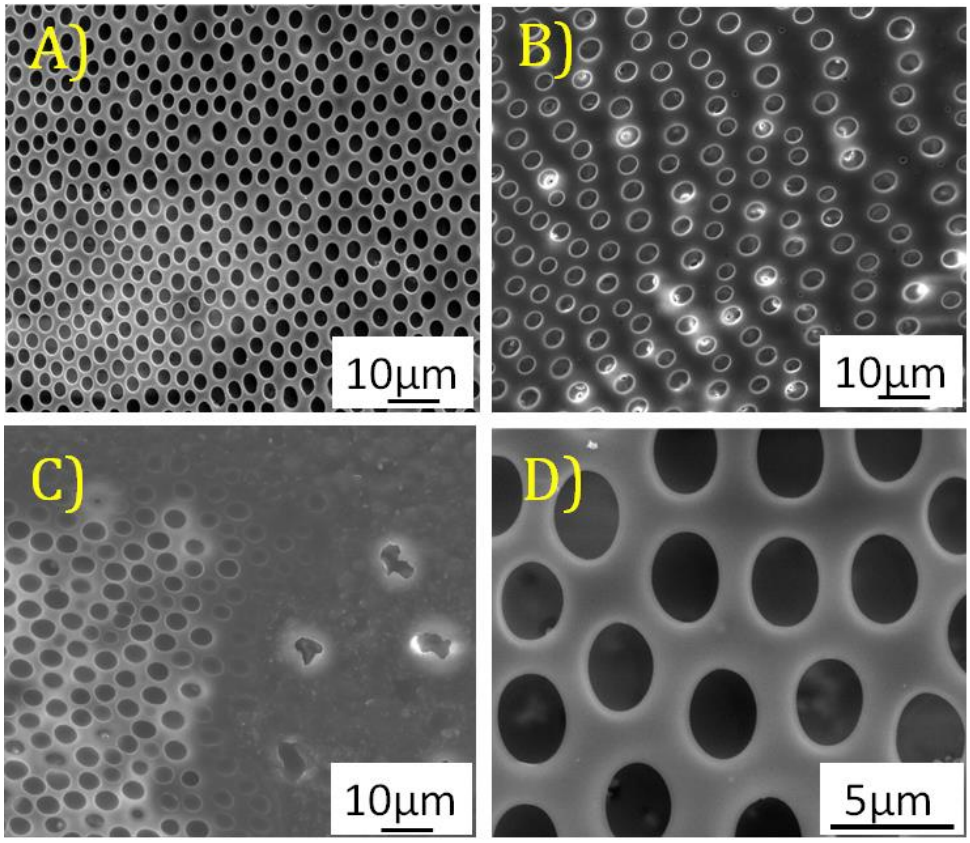

Figure 4.8. SEM images of patterned hybrid film (A) P0.5(3SA20), (B) P1(3SA20), (C) P2(3SA20) and (D) magnified image of (A)

Table 4.3. The average cavity size, feature density and conformational entropy of BF patterns produced on P0.5(SA20) and P3(2.6SA100) films

Sample	Av. cavity Size (µm)	Feature Density (per cm^2)	Conformational Entropy (S)
P0.5(3SA20)	2.85 ± 0.12	5.8× 10^7	0.60
P3(2.6SA100)	1.61 ± 0.09	14x10^7	0.68

Table 4.3 provides a comparison of the cavity size, feature density and conformational entropy of BF patterns produced on P0.5(3SA20) and P3(2.6SA100)

films, where the 3SA20 and 2.6SA100 particles had close value of Hb/Hp balance. The data for P3(2.6SA100) was taken from chapter 3. The data revealed that P3(2.6SA100) exhibited a cavity size 50% less than and a feature density 120% more than that observed for P0.5(3SA20).

The difference in morphology of the patterns due to the different particle size can be explained in terms of the adsorption capability of these particles at the droplet/polymer solution interface. As earlier mentioned, the adsorption energy at the interface is directly related to the particle size according to the equation 4.1. The large BF cavity size and reduced feature density for observed P0.5(3SA20) was due to the lower stabilization capacity of these particles. Reduction in the cavity/droplet size led to enhanced feature density. Increased of particle concentration as in P1(3SA20) and P2(3SA20) led to irregular pattern. XRD of plain films of its counterparts (Figure 4.9) revealed particle agglomeration which became more prominent for P2(3SA20). The agglomeration led to reduction in the effective number of the particle domains in the suspension. This caused increase in droplet size, reduction in number of droplets and loss of pattern regularity. Excessive agglomeration and settling of agglomerates in P2(3SA20) resulted in drastic reduction in the effective number of particle domains and thereby exhibited ill-structured pattern

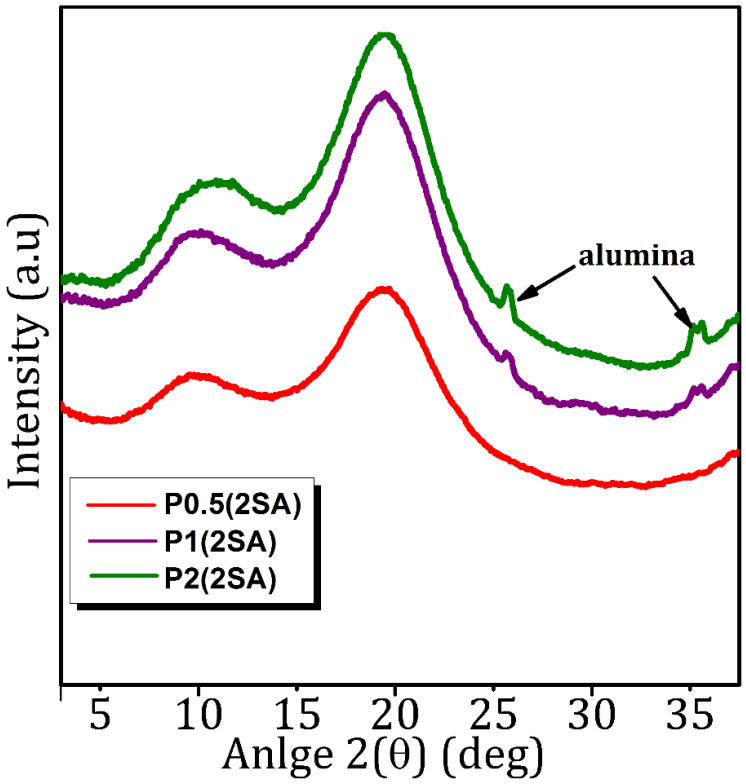

Figure 4.9. XRD patterns of P0.5(3SA20), P1(3SA20), P2(3SA20) films with plain surfaces showing the peaks for alumina for P1(3SA20), P2(3SA20) due to particle agglomeration.

4.3.3. Effect of Polypropylene Substrate on BF Pattern Morphology

Drop cast P3(4SA) hybrid film from suspension of 4SA particles in PS solutions in different solvents were also prepared using polypropylene (PP) sheets as the substrate, employing the experimental conditions for preparing the films using glass substrate. While the suspension in THF failed to yield patterned film, that in CS2 and DCM produced irregular patterns. On the other hand, the suspension in CFM yielded relatively regular breath figure patterns. The drop cast residue was found merged with the substrate since CFM is capable of solvating PP. Figure 4.10 shows the SEM images of BF patterns produced for P3(4SA) hybrid film. The cavity size was larger

(2.2 ±0.13 μm) than of the size (~1.5 μm) produced on the glass substrate. Accumulation of alumina particles in the BF cavity was also observed.

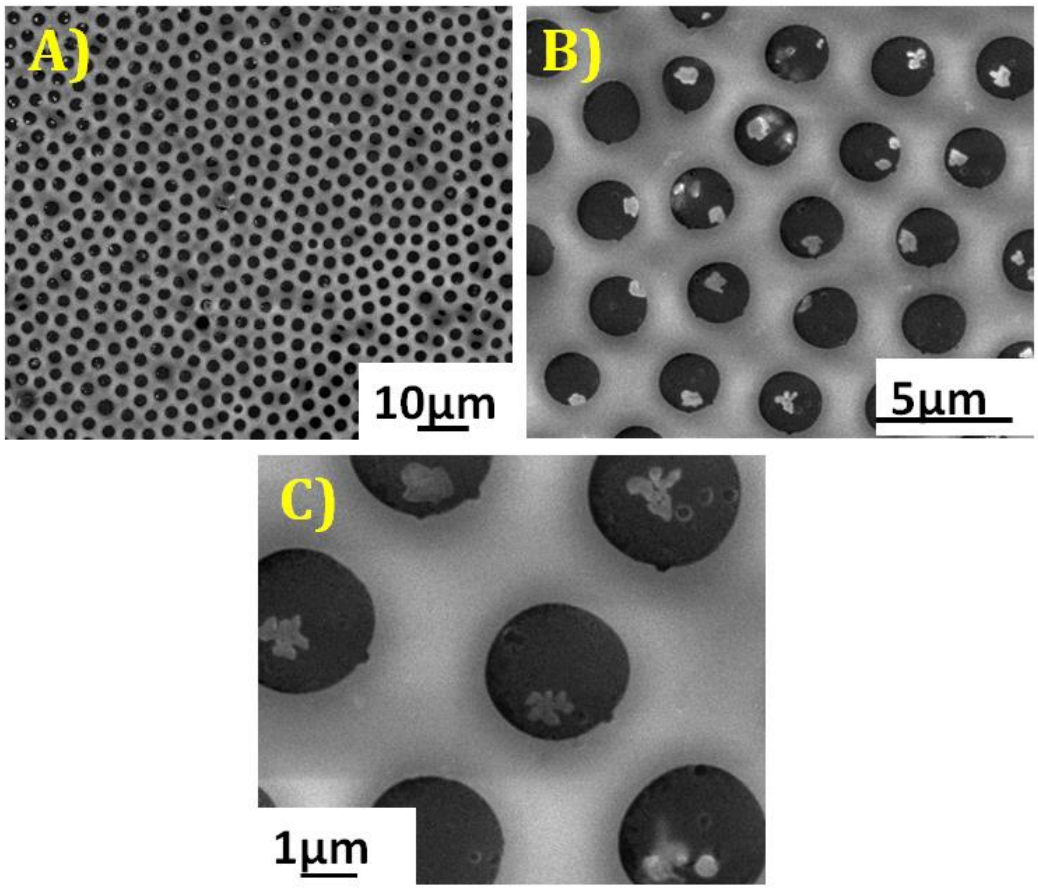

Figure 4.10. SEM images of patterned film prepared using P3(4SA)/ CFM solution by drying the drop cast on PP film surface

There were limited studies on the influence of substrate on the morphology of BF patterns. It has been recognized that the interaction between the substrate and the polymer is beneficial for the periodic arrangement of the pattern. Polypropylene is compatible to a certain extent with PP due to hydrophobic nature. This is manifested by the dissolution of these materials in CFM. This would limit the mobility of precipitated polystyrene layer in contact with the PP substrate. According to Bunz (*Bunz, 2006*), the "polymer-bag effect" or the encapsulation of the water droplets by the precipitated polymer layer is an important criterion in the final stages of droplet

stabilization. The polymer bag cannot easily be assembled around the water droplets due to the interaction between the polymer/solvent/substrate. Therefore, the pore size increased to an average value of 2.2 μm in the case of PP substrate when compared to ~1.5 μm in the case of glass substrate. On the other hand, the amphiphilic alumina particles migrated towards the water droplet/ polymer solution interface readily absorbed in the water phase, possibly due to the incompatible nature of the particles with the PP substrate, a partially miscible substrate. On drying the water droplet, the particles are seen accumulated in the BF cavity.

4.4. CONCLUSION

In conclusion, the influence of the solvent, the particle size as well as the substrate on the breath figure morphology in hybrid films has been demonstrated. The results of studies using tetrahydrofuran (THF), chloroform (CFM), carbon disulphide (CS2) and dichloromethane (DCM) proved that different solvents behaved differently towards the BF formation in the hybrid films. The interaction between the amphiphilic-alumina particles and the solvent was the main factor which determined the BF morphology. Besides, the solvent characteristics such as water miscibility, evaporation rate (vapour pressure) and polarity was also the decisive parameters. All these factors have to be considered to explain the BF morphology using a specific solvent. For examples, while the particles having moderate Hb/Hp balance could produce regular BF pattern from THF, relatively high Hb/Hp value was necessary for the films from CFM and CS2. In DCM, the high interfacial tension between the water droplet and the solvent, and its insensitivity to the particle inclusion in the interface due to strong interaction between the solvent and the particle favoured multilayered

morphology. In the case of non-polar solvents like CFM and CS2, the regularity increased with the hydrophobicity of the particles.

The change particle size had any influence on the regularity of the BF patterns in the hybrid films, but the cavity size increased and the feature density decreased on reducing the particle size. The only advantage was that regular pattern with particles having low size were possible at relatively low concentrations. Of course, particle dispersion loading limit is proportional to the particle size.

In contrast to the observations made on the hydrophilic glass substrate, the BF formation on hydrophobic substrate was solvent specific. For example, while the hybrid system from chloroform yielded regular BF patterns, that from carbon disulphide and dichloromethane produced irregular patterns and no pattern from THF. On the other hand, regular patterns were possible on glass substrate from the above said solvent.